

Exact solution of Schrödinger equation for the complex Morse potential to investigate physical systems with position-dependent complex mass

Partha Sarathi¹ and Bhaskar Singh Rawat²

¹Department of Physics, Maharaja Agrasen College, University of Delhi, Vasundhara Enclave, Delhi-110096, India

²Department of Physics, Hemvati Nandan Bahuguna Garhwal University, Srinagar-246174, Uttarakhand, India

Abstract

This paper presents the exact ground state solution for a diatomic particle system with position-dependent complex mass under action of a complex Morse potential in the quantum domain. By solving the position-dependent Schrödinger equation in extended complex phase space without assuming a specific mass profile, we derive both the eigenfunctions and corresponding eigenenergies using the analyticity conditions of the eigenfunctions. A key focus is placed on addressing the challenge of normalization inherent in non-Hermitian Hamiltonians. To overcome the limitations of conventional normalization methods in systems with complex potentials and spatially varying mass, we propose a modified normalization approach based on a two-dimensional integral over phase space. The results reveal that, under certain parameter constraints, real energy spectra can arise in non-Hermitian settings, supported by normalized and physically meaningful eigenfunctions. Probability density plots validate the existence of stable, localized bound states, maintaining essential characteristics of the traditional Morse potential. Moreover, the model offers potential applications in high-energy and cosmological physics, particularly in the quantum description of exotic systems like dark matter.

Keywords— exact solution, real eigenvalues, complex Morse potential, position-dependent mass, complex mass, bound states, dark matter

1 Introduction

The study of non-Hermitian operators, particularly in the realm of finding the solution of Schrödinger equation with complex potentials, has gained significant attention in last three decades due to its applications in open quantum systems, optical systems, and resonance phenomena. Unlike self-adjoint operators, non-Hermitian operators may possess complex eigenvalues, non-orthogonal eigenfunctions, and lack a complete set of eigenvectors. Foundational contributions by T. Kato [1] laid the groundwork for understanding the spectral properties of non-self-adjoint operators, including spectral instabilities and the emergence of Jordan blocks. E. B. Davies [2] explored pseudospectra and spectral pollution, emphasizing the physical and numerical consequences of non-normal operators. The framework of PT-symmetric and pseudo-Hermitian quantum mechanics, developed by C. M. Bender [3] and A. Mostafazadeh [4] respectively, showed that certain non-Hermitian Hamiltonians can still have entirely real spectra under symmetry constraints. Rigged Hilbert spaces and

¹parthasarathi@mac.du.ac.in

²bhaskarsinghrawat20@gmail.com

Hardy spaces have also been employed to describe decaying states and resonances rigorously, particularly in complex scaling and scattering theory [5]. These developments reveal that the spectral analysis of non-Hermitian systems requires tools beyond the standard Hilbert space formalism and often demands functional analytic techniques tailored to generalized or dissipative operators [6, 7]. Our work aims to position itself within this broader context by incorporating these insights where applicable.

Systems with position-dependent mass have garnered significant interest from researchers in recent decades due to their diverse applications across fundamental areas of physics. These systems can be analyzed from both classical and quantum perspectives. In the quantum domain, recent research has focused on obtaining the solution of the Schrödinger equation with a position-dependent mass, exploring various studies in this area [8–11]. The concept of position-dependent mass has been applied in numerous fields, including semiconductors [12–18], quantum wells and quantum dots [19–25], quantum liquids [26], and impurities in crystals [27], graded mixed semiconductors [28], abrupt heterostructures [29, 30] and in lattice and superlattice systems [31, 32]. Additionally, they play a role in investigating inversion potentials in molecules using density functional theory [33], many-body systems [34], the energy spectrum and transition rates of atomic nuclei [35], magnetic monopoles [36], as well as classical and quantum nonlinear oscillators [37–40] and curved spaces [41].

Further, the investigation of various potentials in the quantum domain with position-dependent mass has increasingly captured the attention of theoretical physicists. Recent studies have explored position-dependent mass carriers in different potential scenarios, such as a 3-dimensional cylindrical wire with a hyperbolic potential [42], an oscillator-shaped quantum well [43], a Pöschl-Teller-type potential [44], and a Morse potential [45].

The Morse potential has been effectively used to describe the vibrational and rotational behaviour of diatomic molecules [46]. Although several studies [47–54] have investigated solutions to the Schrödinger equation with a position-dependent mass for the Morse potential, these approaches typically involve approximation techniques. Such methods often rely on assumptions about the mass function or other parameters of the potential, rather than providing exact solutions to the Schrödinger equation.

Although several efforts have been made to find the solution of the Schrödinger equation for the potential dependent masses, little effort has been allotted to obtain the exact solution for such potentials in the quantum domain. Some efforts have been made to develop a quantum kinetic energy operator within the Schrödinger equation to create a new class of exactly solvable models featuring a position-dependent mass [55], they primarily focus on the real potentials [56, 57]. The study of complex potentials has gathered interest due to their novel properties and their probable applications in the realm of various branches of science to understand the behaviour of complex physical systems. An extended complex phase space formulation of Schrödinger quantum mechanics [58–63] has been employed to study the complex potentials and gain insight into understanding the quantum dynamics of Non-Hermitian Hamiltonian systems (NHH) systems. The same formulation was used to establish that it is indeed feasible for negative masses for various physical systems to be bound together by complex Morse potential. It was established that atoms with negative masses may bind together under the action of complex Morse-like potentials and form molecular structures [64]. Furthermore, in the domain of relativistic quantum mechanics, Özlem et.al [65] arrived at the solution of the Dirac equation in the frame of position-dependent mass where the eigenvalues of the Dirac operator for the complex Morse and trigonometric complex Scarf-II potentials $SL(2, C)$ using Lie algebras and the supersymmetric quantum mechanical approaches were obtained.

The study of dark matter in the realm of Cosmology and Quantum Mechanics poses serious

challenges as the only concrete evidence for dark matter (DM) stems from its gravitational interactions. Determining the nature of DM is one of the principal challenges of modern experimental physics. The theoretical investigations of position dependent masses in the quantum domain have opened new vistas for arriving at a plausible theory to explain the characteristics of the DM. The system of stability equations for galactic halos is under-determined in most of the models of dark matter (DM) which has been conventionally resolved by taking the temperature as a constant, and the chemical potential and the mass density as position-dependent variables [66]. The position-dependent probability distribution function (PDF) of the smoothed matter field as a cosmological observable was introduced to highlight position-dependent PDF and its distinct dependence on cosmological parameters [67]. By considering the diffusion coefficient as increasing exponentially with the distance from the disk, it was established that the antiproton flux predicted deviates from the conventional calculation for the same dark matter parameters by up to about 25% [68]. A study of the position-dependent Voronoi density PDF, measured within finite subregions of the Universe, using separate universe simulations, demonstrate that the spatial variation of the position-dependent PDF is due to large-scale density fluctuations [69]. Brax et.al [70] explored alternatives to the collisionless cold dark matter paradigm by proposing a simple two-component dark matter model that features derivative conformal interactions between the two DM species. In their model, they considered temperature and the chemical potential as position-dependent variables. Other studies have forwarded arguments in favor of the mass-dependent maximal acceleration (MDMA) by proposing a hypothesis that there exists a maximal force with the numerical value equal to the inverse Einstein's gravitation constant [71]. Attempt has been made recently to prove that the molecules in the dark matter which are assumed to be negative complex masses can bind together under the action of complex Morse-like potentials and form molecular structures [64].

With the explanation of dark matter still an open problem, an attempt is made in this paper to study the position-dependent complex mass (PDCM) under action of complex morse potential in the quantum domain. Further, the results obtained are analyzed to forward a quantum mechanical explanation of the composition of dark matter. We propose that the dark matter can be a PDCM under the action of complex Morse potential. Thus, we find the exact solution of the Schrödinger equation for the one-dimensional complex Morse potential with PDCM,

$$V(x) = V_0 [e^{-2ax} - 2e^{-ax}].$$

where V_0 is the well depth, x is the internuclear distance (bond length), $x > 0$ and a is related to the vibrational constant μ as

$$a = \pi\mu\sqrt{\frac{2M}{V_0}}.$$

The reduced mass M of the system is considered a position-dependent mass and is a function of the internuclear distance x which is taken as complex. In general, the parameters V_0 and a are also considered complex as the objective of the study is to investigate the bonding between two particles of PDCM.

The arrangement of the paper is as follows: In Section 2, a general formulation for the solution of the Schrödinger equation for a general class of complex potential is enumerated. In Section 3, the exact solution of the Schrödinger equation is obtained for the general class of one-dimensional complex Morse potential with PDCM and its eigenvalues and eigenfunction are computed. Further the normalized eigenfunction and probability density is derived in Section 4. The exact solution of normalized eigenfunction and eigenvalues are implemented in Section 5 for the general case of

PDCM. The admissibility of real eigenvalues is discussed in Section 6. Lastly, a general discussion on the results and applications of such studies is carried forward in Section 7.

2 Schrödinger equation for PDM and its general solution

This paper aims to investigate the quantum behaviour of a diatomic particle system with a position-dependent complex mass under the influence of a complex Morse potential. By solving the position-dependent Schrödinger equation (PDMSE) for the above-mentioned potential in extended complex phase space, we obtain exact ground-state eigenfunctions and energies. Unlike previous attempts in the literature to solve the Schrodinger equation for position-dependent real Morse potentials, no specific mass profile is assumed. The approach relies on analyticity conditions to ensure physical solutions that can also admit real energy spectra under certain constraining relations amongst the potential parameters. This framework reveals that position-dependent complex mass systems admit normalized eigenfunctions and can support bound states, expanding the scope of quantum models that can be applied in various physical systems like quantum dots, quantum wells, dark matter etc.

The solution to the position-dependent mass Schrödinger equation (PDMSE) can be expressed by reformulating the position x and momentum p in complex phase space, which is increasingly advocated in recent years due to its potentially more rigorous mathematical foundation, as given by [72]

$$x = x_1 + ip_2, \quad p = p_1 + ix_2. \quad (1)$$

where the imaginary parts x_2 and p_2 introduced in the variables p and x turn out to be canonical pairs of p_1 and x_1 respectively. The complexification of phase space enumerated in eq (1), wherein the canonical variables provide a range of significant advantages that enhance both the analytical tractability and physical understanding of the quantum systems. This formulation of extended complex phase space is particularly useful for non-Hermitian systems where both the potential and the effective mass function are complex, as is the case in our study of exact solutions to the Schrödinger equation with a complex Morse potential. By extending the phase space into the complex domain, one gains access to analytic techniques such as Cauchy–Riemann conditions, which decompose the complex Hamiltonian into two real components that correspond to a coupled real system, allowing a deeper investigation into integrability and dynamical structure that may remain obscured in purely real formulations. The analyticity through the Cauchy–Riemann conditions on the complex Hamiltonian also reveal hidden symmetries in the two coupled real systems. Furthermore, the real and imaginary parts of the eigenfunctions and eigenspectra can be obtained explicitly, which is not the case with any other methods applied in the literature. This aids in exploring the conditions of admitting the reality of eigenspectra for Complex potentials and investigation of their behaviour. Thus, complexifying phase space not only enriches the mathematical structure of the problem but also serves as a powerful tool for uncovering exact solvability, hidden symmetries, and physical insight in systems with complex potentials and non-trivial mass structures. Equation 1 can be applied to recast the analogous Schrödinger equation (ASE) in terms of x_1 and p_2 ,

$$\hat{H}(x, p)\psi(x) = E\psi(x). \quad (2)$$

where

$$H(x, p) = -\frac{\hbar^2}{2M} \frac{\partial^2}{\partial x^2} + V(x). \quad (3)$$

and $V(x)$ is a complex potential. Note that since equation 2 departs from the conventional conceptual and mathematical setting of the standard Schrodinger equation, we call equation the 'analogous Schrodinger equation' (ASE) for the non-Hermitian operator $H(x, p)$.

If the mass is considered as position dependent, the Schrödinger equation 2 can be written in the following form [12]

$$-\frac{\hbar^2}{2M} \left(\frac{\partial^2}{\partial x^2} - \frac{1}{M} \frac{\partial M}{\partial x} \frac{\partial}{\partial x} \right) \psi(x) = (E - V(x))\psi(x). \quad (4)$$

In the quantum context, since $p \rightarrow -i\hbar \frac{\partial}{\partial x}$ which implies $p_1 \rightarrow -\frac{\partial}{\partial p_2}$, $x_2 \rightarrow \frac{\partial}{\partial x_1}$, the analyticity of $H(x,p)$ gets translated into that of the complex potential function $\tilde{V}(x)$.

Writing the wavefunction, potential and the energy eigenvalues in real and imaginary part as

$$\psi(x) = \psi_r(x_1, p_2) + i\psi_i(x_1, p_2), \quad V(x) = V_r(x_1, p_2) + iV_i(x_1, p_2), \quad E = E_r + iE_i. \quad (5a)$$

and considering the mass as a complex quantity with positive real part of the form

$$M = m_r + im_i, \quad m_r > 0, \quad (5b)$$

$$\frac{1}{M} = \frac{1}{m_r + im_i} = \frac{m_r - im_i}{m^2}. \quad (5c)$$

where the subscript r and i respectively denote the real and imaginary parts of the corresponding physical quantity. Thus, using equations 5a-5c and employing the analytical property of the wave function $\psi(x)$ and the mass M in terms of Cauchy-Riemann condition, namely

$$\psi_{r,x_1} = \psi_{i,p_2}; \quad \psi_{r,p_2} = -\psi_{i,x_1}, \quad (6a)$$

$$m_{r,x_1} = m_{i,p_2}; \quad m_{r,p_2} = -m_{i,x_1}. \quad (6b)$$

The partial derivative of x can thus be expressed in the form of x_1 and p_2 as

$$\frac{\partial}{\partial x} = \frac{1}{2} \left(\frac{\partial}{\partial x_1} - i \frac{\partial}{\partial p_2} \right), \quad (7a)$$

$$\frac{\partial^2}{\partial x^2} = \frac{1}{4} \left(\frac{\partial^2}{\partial x_1^2} - \frac{\partial^2}{\partial p_2^2} \right) - \frac{i}{2} \frac{\partial^2}{\partial x_1 \partial p_2}. \quad (7b)$$

Substituting the equations 7a, 7b, in equation 4

$$-\frac{\hbar^2}{2M} \left\{ \frac{1}{4} \left(\frac{\partial^2}{\partial x_1^2} - \frac{\partial^2}{\partial p_2^2} \right) - \frac{i}{2} \frac{\partial^2}{\partial x_1 \partial p_2} - \frac{1}{M} \frac{\partial M}{\partial x} \frac{\partial}{\partial x} \right\} \psi(x) = (E - V(x))\psi(x).$$

Putting the value of mass M from 5c in the above equation, we arrive at the following:

$$\begin{aligned} & -\frac{\hbar^2}{2m^2} \left[\left\{ \frac{m_r}{4} \left(\frac{\partial^2}{\partial x_1^2} - \frac{\partial^2}{\partial p_2^2} \right) - \frac{m_i}{2} \frac{\partial^2}{\partial x_1 \partial p_2} \right\} - i \left\{ \frac{m_i}{4} \left(\frac{\partial^2}{\partial x_1^2} - \frac{\partial^2}{\partial p_2^2} \right) + \frac{m_r}{2} \frac{\partial^2}{\partial x_1 \partial p_2} \right\} \right] \psi(x) \\ & + \frac{\hbar}{4m^4} \left[(m_r - im_i)^2 \frac{\partial}{\partial x_1} (m_r + im_i) \left(\frac{\partial}{\partial x_1} - i \frac{\partial}{\partial p_2} \right) \right] \psi(x) = [(E_r - V_r)\psi_r - (E_i \\ & - V_i)\psi_i] + i [(E_i - V_i)\psi_r + (E_r - V_r)\psi_i]. \end{aligned} \quad (8)$$

Solving equation 8, we get

$$\begin{aligned} \Rightarrow & -\frac{\hbar^2}{2m^2} [(m_r\psi_r'' + m_i\psi_i'') + i(m_r\psi_i'' - m_i\psi_r'')] + \frac{\hbar^2}{2m^4} [\{(m_r^2 - m_i^2)(m_r'\psi_r' - m_i'\psi_i') \\ & + 2m_r m_i(m_i'\psi_r' + m_r'\psi_i')\}] + \frac{\hbar^2}{2m^4} [i\{(m_r^2 - m_i^2)(m_i'\psi_r' + m_r'\psi_i') - 2m_r m_i(m_r'\psi_r' \\ & - m_i'\psi_i')\}] = ((E_r - V_r)\psi_r - (E_i - V_i)\psi_i) + i((E_i - V_i)\psi_r + (E_r - V_r)\psi_i). \end{aligned} \quad (9)$$

The real and imaginary parts of the L.H.S. of equation 9 can be obtained as

$$\frac{\hbar^2}{2m^4}[-m^2(m_r\psi_r'' + m_i\psi_i'') + (m_r^2 - m_i^2)(m_r'\psi_r' - m_i'\psi_i') + 2m_r m_i(m_i'\psi_r' + m_r'\psi_i')]. \quad (10a)$$

$$\frac{\hbar^2}{2m^4}[-m^2(m_r\psi_i'' - m_i\psi_r'') + (m_r^2 - m_i^2)(m_i'\psi_r' + m_r'\psi_i') - 2m_r m_i(m_r'\psi_r' - m_i'\psi_i')]. \quad (10b)$$

Defining the values of functions A,B,C,D as

$$A = m_r\psi_r'' + m_i\psi_i'',$$

$$B = m_r\psi_i'' - m_i\psi_r'',$$

$$C = m_r'\psi_r' - m_i'\psi_i',$$

$$D = m_i'\psi_r' + m_r'\psi_i'.$$

and substituting them in equations 10a and 10b, we arrive at following equations:

$$\Rightarrow \frac{\hbar^2}{2m^4}[-m^2A + (m_r^2 - m_i^2)C + 2m_r m_i D] = [E_r\psi_r - E_i\psi_i - V_r\psi_r + V_i\psi_i] \quad (11a)$$

and

$$\Rightarrow \frac{\hbar^2}{2m^4}[-m^2B + (m_r^2 - m_i^2)D - 2m_r m_i C] = [E_i\psi_r + E_r\psi_i - V_i\psi_r - V_r\psi_i]. \quad (11b)$$

Employing the eigenfunction-ansatz method, the coupled equations 11a and 11b are solved by taking the ansatz for the eigenfunction as

$$\psi(x) = \phi(x)e^{ig(x)}. \quad (12a)$$

For obtaining the solution for the ground state, we substitute

$$\phi(x) = 1.$$

Thus,

$$\psi_r + i\psi_i = e^{i(g_r + ig_i)} = e^{-g_i}(\cos g_r + i \sin g_r). \quad (12b)$$

Which implies

$$\psi_r = e^{-g_i} \cos g_r; \quad \psi_i = e^{-g_i} \sin g_r. \quad (12c)$$

Equation 11a can be recast as

$$\begin{aligned} & \frac{\hbar^2}{2m^4} \left[-m^2 \{ m_r e^{-g_i} (g_i'^2 \cos g_r - g_r'^2 \cos g_r - g_i'' \cos g_r - g_r'' \sin g_r + 2g_r' g_i' \sin g_r) \right. \\ & + m_i e^{-g_i} (g_i'^2 \sin g_r - g_r'^2 \sin g_r + g_r'' \cos g_r - g_i'' \sin g_r - 2g_r' g_i' \cos g_r) \} + (m_r^2 - m_i^2) \\ & \left. \{ m_r' e^{-g_i} (-g_i' \cos g_r - g_r' \sin g_r) - m_i' e^{-g_i} (g_r' \cos g_r - g_i' \sin g_r) \} + \right. \\ & \left. 2m_i m_r \{ m_i' e^{-g_i} (-g_i' \cos g_r - g_r' \sin g_r) + m_r' e^{-g_i} (g_r' \cos g_r - g_i' \sin g_r) \} \right] = E_r e^{-g_i} \cos g_r \\ & - V_r e^{-g_i} \cos g_r - E_i e^{-g_i} \sin g_r + V_i e^{-g_i} \sin g_r. \end{aligned} \quad (13)$$

Equating the coefficient of $\cos g_r$ and $\sin g_r$ term from the equation 13, one obtains first set of coupled equations as

$$\frac{\hbar^2}{2m^4} [-m^2 \{m_r(g_i'^2 - g_r'^2 - g_i'') + m_i(g_r'' - 2g_r'g_i')\} + (m_r^2 - m_i^2) \{-m_r'g_i' - m_i'g_r'\} + 2m_r m_i \{m_r'g_r' - m_i'g_i'\}] = E_r - V_r, \quad (14a)$$

$$\frac{\hbar^2}{2m^4} [-m^2 \{m_r(-g_r'' + 2g_r'g_i') + m_i(g_i'^2 - g_r'^2 - g_i'')\} + (m_r^2 - m_i^2) \{-m_r'g_r' + m_i'g_i'\} + 2m_r m_i \{-m_i'g_r' - m_r'g_i'\}] = -E_i + V_i. \quad (14b)$$

Similarly, substituting the values of A,B,C and D in the equation 11b, we get

$$\begin{aligned} & \frac{\hbar^2}{2m^4} [-m^2 \{m_r e^{-g_i} (g_i'^2 \sin g_r - g_r'^2 \sin g_r + g_r'' \cos g_r - g_i'' \sin g_r - 2g_r'g_i' \cos g_r) - \\ & m_i e^{-g_i} (g_i'^2 \cos g_r - g_r'^2 \cos g_r - g_i'' \cos g_r - g_r'' \sin g_r + 2g_r'g_i' \sin g_r)\} + \\ & (m_r^2 - m_i^2) \{m_i' e^{-g_i} (-g_i' \cos g_r - g_r' \sin g_r) + m_r' e^{-g_i} (g_r' \cos g_r - g_i' \sin g_r)\} - \\ & 2m_i m_r \{m_r' e^{-g_i} (-g_i' \cos g_r - g_r' \sin g_r) - m_i' e^{-g_i} (g_r' \cos g_r - g_i' \sin g_r)\}] = E_i e^{-g_i} \cos g_r \\ & - V_i e^{-g_i} \cos g_r + E_r e^{-g_i} \sin g_r - V_r e^{-g_i} \sin g_r. \end{aligned} \quad (15)$$

Again, equating the coefficients of $\cos g_r$ and $\sin g_r$ terms respectively from equation 15, one obtains second set of coupled equations, namely

$$\frac{\hbar^2}{2m^4} [-m^2 \{m_r(-g_r'' + 2g_r'g_i') + m_i(g_i'^2 - g_r'^2 - g_i'')\} + (m_r^2 - m_i^2) \{-m_r'g_r' + m_i'g_i'\} + 2m_r m_i \{-m_i'g_r' - m_r'g_i'\}] = -E_i + V_i, \quad (16a)$$

$$\frac{\hbar^2}{2m^4} [-m^2 \{m_r(g_i'^2 - g_r'^2 - g_i'') + m_i(g_r'' - 2g_r'g_i')\} + (m_r^2 - m_i^2) \{-m_r'g_i' - m_i'g_r'\} + 2m_r m_i \{m_r'g_r' - m_i'g_i'\}] = E_r - V_r. \quad (16b)$$

The coupled equations 16a and 16b can be solved for any complex potential by substituting the values of real and imaginary part of the given potential and taking suitable ansatz for the real and imaginary part of function $g(x)$ enumerated in equation 12a. In this study we wish to solve the coupled equations for complex Morse potential with PDCM.

3 Complex Morse potential with position-dependent complex mass

In this section, the solution of ASE 4 for the complex Morse potential

$$V(x) = V_0 [e^{-2ax} - 2e^{-ax}] . (V_0, a \text{ complex}) \quad (17a)$$

is calculated in terms of parameters of extended phase space. The real and imaginary part of the potential 17a can be expressed as

$$\begin{aligned} V_r(x_1, p_2) &= V_{0r} [e^{-2X} \cos 2Y - 2e^{-X} \cos Y] + V_{0i} [e^{-2X} \sin 2Y - 2e^{-X} \sin Y], \\ V_i(x_1, p_2) &= V_{0i} [e^{-2X} \cos 2Y - 2e^{-X} \cos Y] - V_{0r} [e^{-2X} \sin 2Y - 2e^{-X} \sin Y]. \end{aligned} \quad (17b)$$

where $X = a_r x_1 - a_i p_2$; $Y = a_i x_1 + a_r p_2$; $V_0 = V_{0r} + iV_{0i}$ and $a = a_r + ia_i$ are used.

The ansatz of the eigenfunction is taken in the form

$$\begin{aligned} g_r(x_1, p_2) &= \beta_1 x_1 - \alpha_1 p_2 + \beta_3 e^{-X} \cos Y, \\ g_i(x_1, p_2) &= \alpha_1 x_1 + \beta_1 p_2 - \beta_3 e^{-X} \sin Y. \end{aligned} \quad (18)$$

Substituting the partial derivatives of ansatz of the eigenfunction in 14a and 14b we get

$$\begin{aligned} &\frac{\hbar^2}{2m^4} [-m^2 \{m_r (\alpha_1^2 - \beta_1^2 - e^{-2X} \cos 2Y \beta_3^2 (a_r^2 - a_i^2) + e^{-X} \sin Y (2\alpha_1 \beta_3 a_r + 2\beta_1 \beta_3 a_i \\ &+ \beta_3 (a_r^2 - a_i^2)) + e^{-X} \cos Y (-2\alpha_1 \beta_3 a_i + 2\beta_3 \beta_1 a_r - 2\beta_3 a_r a_i) - 2\beta_3^2 a_r a_i e^{-2X} \sin 2Y) \\ &+ m_i (-2\alpha_1 \beta_1 + e^{-X} \cos Y (2\beta_1 \beta_3 a_i + 2\alpha_1 \beta_3 a_r + \beta_3 (a_r^2 - a_i^2)) e^{-X} \sin Y (2\alpha_1 \beta_3 a_i - \\ &+ 2\beta_1 \beta_3 a_r + 2\beta_3 a_r a_i) + e^{-2X} \sin 2Y \beta_3^2 (a_r^2 - a_i^2) - 2e^{-2X} \cos 2Y \beta_3^2 a_r a_i\} - (m_r^2 - m_i^2) \\ &\{m'_i \beta_1 + m'_r \alpha_1 - e^{-X} \cos Y (m'_i \beta_3 a_r + m'_r \beta_3 a_i) - e^{-X} \sin Y (m'_i \beta_3 a_i - m'_r \beta_3 a_r)\} + 2m_r m_i \\ &\{m'_r \beta_1 - m'_i \alpha_1 - e^{-X} \cos Y (m'_r \beta_3 a_r - m'_i \beta_3 a_i) - e^{-X} \sin Y (m'_r \beta_3 a_i + m'_i \beta_3 a_r)\}] = E_r \\ &- V_{0r} (e^{-2X} \cos 2Y - 2e^{-X} \cos Y) - V_{0i} (e^{-2X} \sin 2Y - 2e^{-X} \sin Y) \end{aligned} \quad (19)$$

and,

$$\begin{aligned} &\frac{\hbar^2}{2m^4} [-m^2 \{m_r (-2\alpha_1 \beta_1 + e^{-X} \cos Y (2\beta_1 \beta_3 a_i + 2\alpha_1 \beta_3 a_r + \beta_3 (a_r^2 - a_i^2)) + e^{-X} \sin Y \\ &(2\alpha_1 \beta_3 a_i - 2\beta_1 \beta_3 a_r + 2\beta_3 a_r a_i) + e^{-2X} \sin 2Y (\beta_3^2 (a_r^2 - a_i^2)) - 2\beta_3^2 a_r a_i e^{-2X} \cos 2Y) + m_i \\ &(-\alpha_1^2 + \beta_1^2 + e^{-2X} \sin 2Y (2a_r a_i \beta_3^2) + e^{-2X} \cos 2Y (\beta_3^2 (a_r^2 - a_i^2)) + e^{-X} \sin Y (-2\alpha_1 \beta_3 a_r - \\ &2\beta_1 \beta_3 a_i - \beta_3 (a_r^2 - a_i^2)) + e^{-X} \cos Y (2\alpha_1 \beta_3 a_i - 2\beta_3 \beta_1 a_r + 2\beta_3 a_r a_i) - 2\beta_3^2 a_r a_i e^{-2X} \sin 2Y)\} \\ &+ (m_r^2 - m_i^2) \{m'_r \beta_1 - m'_i \alpha_1 - e^{-X} \cos Y (m'_r \beta_3 a_r - m'_i \beta_3 a_i) - e^{-X} \sin Y (m'_r \beta_3 a_i + m'_i \beta_3 a_r)\} \\ &+ 2m_r m_i \{m'_i \beta_1 + m'_r \alpha_1 - e^{-X} \cos Y (m'_i \beta_3 a_r + m'_r \beta_3 a_i) - e^{-X} \sin Y (m'_i \beta_3 a_i - m'_r \beta_3 a_r)\}] \\ &= E_i - V_{0i} [e^{-2X} \cos 2Y - 2e^{-X} \cos Y] + V_{0r} [e^{-2X} \sin 2Y - 2e^{-X} \sin Y]. \end{aligned} \quad (20)$$

Comparing both side constant terms, coefficients of $e^{-X} \cos Y$, $e^{-X} \sin Y$, $e^{-2X} \cos 2Y$, $e^{-2X} \sin 2Y$ of equation 19 and 20 respectively, we get the following non-repeating set of equations as:

$$\begin{aligned} &\frac{\hbar^2}{2m^4} [-m^2 \{m_r (\alpha_1^2 - \beta_1^2) + m_i (-2\alpha_1 \beta_1)\} - (m_r^2 - m_i^2) \{m'_i \beta_1 + m'_r \alpha_1\} + 2m_r m_i \\ &\{m'_r \beta_1 - m'_i \alpha_1\}] = E_r, \end{aligned} \quad (21a)$$

$$\begin{aligned} &\frac{\hbar^2}{2m^4} [-m^2 \{m_r (-2\alpha_1 \beta_1) - m_i (\alpha_1^2 - \beta_1^2)\} + (m_r^2 - m_i^2) \{m'_r \beta_1 - m'_i \alpha_1\} + 2m_r m_i \\ &\{m'_i \beta_1 + m'_r \alpha_1\}] = E_i, \end{aligned} \quad (21b)$$

$$\begin{aligned} &\frac{\hbar^2}{2m^4} [-m^2 \{m_r (-2\alpha_1 \beta_3 a_i + 2\beta_3 \beta_1 a_r - 2\beta_3 a_r a_i) + m_i (2\alpha_1 \beta_3 a_r + 2\beta_3 \beta_1 a_i + \beta_3 (a_r^2 - a_i^2)) + \\ &(m_r^2 - m_i^2) (m'_i \beta_3 a_r + m'_r \beta_3 a_i) - 2m_r m_i (m'_r \beta_3 a_r - m'_i \beta_3 a_i)\}] = 2V_{0r}, \end{aligned} \quad (21c)$$

$$\begin{aligned} &\frac{\hbar^2}{2m^4} [-m^2 \{m_r (2\alpha_1 \beta_3 a_r + 2\beta_1 \beta_3 a_i + \beta_3 (a_r^2 - a_i^2)) + m_i (2\alpha_1 \beta_3 a_i - 2\beta_3 \beta_1 a_r + 2\beta_3 a_r a_i) + \\ &(m_r^2 - m_i^2) \{-m'_r \beta_3 a_r + m'_i \beta_3 a_i\} - 2m_r m_i (m'_i \beta_3 a_r + m'_r \beta_3 a_i)\}] = 2V_{0i}, \end{aligned} \quad (21d)$$

$$\frac{\hbar^2}{2m^4} [-m^2 \{m_r (-2\beta_3^2 a_r a_i) + m_i (\beta_3^2 (a_r^2 - a_i^2))\}] = -V_{0i}, \quad (21e)$$

$$\frac{\hbar^2}{2m^4} [-m^2 \{m_r (-\beta_3^2 (a_r^2 - a_i^2)) + m_i (-2\beta_3^2 a_r a_i)\}] = -V_{0r}. \quad (21f)$$

From equation 21e and 21f we obtain value of β_3 as

$$\beta_3 = \left[\frac{2m^2 V_{0r}}{\hbar^2 [m_r (a_r^2 - a_i^2) + 2m_i a_r a_i]} \right]^{1/2}, \quad (22a)$$

that provides us the constraining relation among the potential parameters, namely,

$$\frac{V_{0i}}{V_{0r}} = \frac{2m_r a_r a_i - m_i (a_r^2 - a_i^2)}{m_r (a_r^2 - a_i^2) + 2m_i a_r a_i}. \quad (22b)$$

Further, equation 21c and 21d can be solved for β_1 and α_1 to give

$$\beta_1 = \beta_3 a_r + \frac{a_i}{2} + \frac{1}{2m^4} [(m_r^2 - m_i^2)(m_r m_i)' + 2m_r m_i (m_i m_i' - m_r m_r')], \quad (23a)$$

$$\alpha_1 = \beta_3 a_i - \frac{a_r}{2} + \frac{1}{2m^4} [(m_r^2 - m_i^2)(m_i m_i' - m_r m_r') - 2m_r m_i (m_r m_i)']. \quad (23b)$$

Defining values of J and K as function of masses and its derivatives,

$$K = [(m_r^2 - m_i^2)(m_r m_i)' + 2m_r m_i (m_i m_i' - m_r m_r')],$$

$$J = [(m_r^2 - m_i^2)(m_i m_i' - m_r m_r') - 2m_r m_i (m_r m_i)'].$$

The value of α_1 and β_1 in terms of J and K can be recast as

$$\beta_1 = \beta_3 a_r + \frac{a_i}{2} + \frac{K}{2m^4}, \quad (24a)$$

$$\alpha_1 = \beta_3 a_i - \frac{a_r}{2} + \frac{J}{2m^4}. \quad (24b)$$

Using the results for β_1 and α_1 , we obtain the expression for the real and imaginary part of energy eigenvalue as

$$\begin{aligned} E_r = \frac{\hbar^2}{2m^4} \left[-m^2 \left\{ m_r \left(\left(\frac{1}{4} - \beta_3^2 \right) (a_r^2 - a_i^2) + \frac{1}{4m^8} (J^2 - K^2) + \beta_3 \left(\frac{J a_i - K a_r}{m^4} - 2a_r a_i \right) \right. \right. \right. \\ \left. \left. - \frac{1}{2m^4} (J a_r + K a_i) \right) - m_i \left(\frac{a_r a_i}{2} (4\beta_3^2 - 1) + \beta_3 (a_r^2 - a_i^2) + \frac{\beta_3}{m^4} (J a_r + K a_i) + \frac{1}{2m^4} (J a_i \right. \right. \\ \left. \left. - K a_r) + \frac{JK}{2m^8} \right) \right\} - (m_r^2 - m_i^2) \left\{ m_i' \left(\beta_3 a_r + \frac{a_i}{2} + \frac{K}{2m^4} \right) + m_r' \left(\beta_3 a_i - \frac{a_r}{2} + \frac{J}{2m^4} \right) \right\} \\ \left. + 2m_r m_i \left\{ m_r' \left(\beta_3 a_r + \frac{a_i}{2} + \frac{K}{2m^4} \right) - m_i' \left(\beta_3 a_i - \frac{a_r}{2} + \frac{J}{2m^4} \right) \right\} \right], \quad (25a) \end{aligned}$$

$$\begin{aligned} E_i = \frac{\hbar^2}{2m^4} \left[-m^2 \left\{ -m_r \left(\frac{a_r a_i}{2} (4\beta_3^2 - 1) + \beta_3 (a_r^2 - a_i^2) + \frac{\beta_3}{m^4} (J a_r + K a_i) + \frac{1}{2m^4} (J a_i \right. \right. \right. \\ \left. \left. - K a_r) + \frac{JK}{2m^8} \right) - m_i \left(\left(\frac{1}{4} - \beta_3^2 \right) (a_r^2 - a_i^2) + \frac{1}{4m^8} (J^2 - K^2) + \beta_3 \left(\frac{J a_i - K a_r}{m^4} - 2a_r a_i \right) \right. \right. \\ \left. \left. - \frac{1}{2m^4} (J a_r + K a_i) \right) \right\} + (m_r^2 - m_i^2) \left\{ m_r' \left(\beta_3 a_r + \frac{a_i}{2} + \frac{K}{2m^4} \right) - m_i' \left(\beta_3 a_i - \frac{a_r}{2} + \frac{J}{2m^4} \right) \right\} \\ \left. + 2m_r' m_i' \left\{ m_i' \left(\beta_3 a_r + \frac{a_i}{2} + \frac{K}{2m^4} \right) + m_r' \left(\beta_3 a_i - \frac{a_r}{2} + \frac{J}{2m^4} \right) \right\} \right]. \quad (25b) \end{aligned}$$

And the eigenfunction is expressed into the following form as

$$\psi = \exp \left[\left\{ \left(\frac{1}{2} + i\beta_3 \right) a - \frac{J - iK}{2m^4} \right\} x + i\beta_3 e^{-ax} \right]. \quad (26)$$

4 Condition for normalized eigenfunction and probability density

The normalization of the eigenfunction of the PDCM system with complex Morse's potential, like other non-Hermitian quantum systems, is still an open problem and subject of research and discussion in the literature. The normalized eigenfunction for the said potential can be written from eq26 as

$$\psi(x) = N \exp \left[\left\{ \left(\frac{1}{2} + i\beta_3 \right) a - \frac{J - iK}{2m^4} \right\} x + i\beta_3 e^{-ax} \right] \quad (27)$$

Where, N is the normalization constant.

The condition for the normalization of eigenfunction can be expressed as,

$$\int_{-\infty}^{\infty} \int_{-\infty}^{\infty} N^2 \psi^*(x_1, p_2) \psi(x_1, p_2) dx_1 dp_2 = N^2 \int_{-\infty}^{\infty} \int_{-\infty}^{\infty} |\psi(x_1, p_2)|^2 dx_1 dp_2 = 1 \quad (28)$$

where, $\psi^*(x_1, p_2)$ represents the complex conjugate of the eigenfunction.

The integral defined in equation 28 can be reduced in terms α_1 and β_1 as,

$$N^2 \int_{-\infty}^{\infty} \int_{-\infty}^{\infty} |\psi(x_1, p_2)|^2 dx_1 dp_2 = N^2 \int_{-\infty}^{\infty} \int_{-\infty}^{\infty} \exp[-2\{\alpha_1 x_1 + \beta_1 p_2\}] dx_1 dp_2 = 1. \quad (29)$$

The above two dimensional integral is divergent for the range of x_1 and p_2 in the region $(-\infty, \infty)$. It is interesting to observe that the above integral converges only for the absolute values of x_1 and p_2 provided both α_1 and β_1 are considered positive values. Thus, by considering x_1 and p_2 as absolute values, and putting the value of integrals

$$\int_{-\infty}^{\infty} \exp[-2\{\alpha_1 |x_1|\}] dx_1 = \frac{1}{\alpha_1}, \quad \int_{-\infty}^{\infty} \exp[-2\{\beta_1 |p_2|\}] dp_2 = \frac{1}{\beta_1}; \quad \alpha_1 > 0, \beta_1 > 0$$

the two dimensional integral in equation 29 takes the form,

$$N^2 \int_{-\infty}^{\infty} \int_{-\infty}^{\infty} |\psi(x_1, p_2)|^2 dx_1 dp_2 = N^2 \frac{1}{\alpha_1 \beta_1} = 1. \quad (30)$$

Which implies that the normalization constant is,

$$N = (\alpha_1 \beta_1)^{\frac{1}{2}}. \quad (31)$$

The constraints on value of both α_1 and β_1 to admit positive values can be recast in terms of β_3 as,

$$\beta_3 > -\frac{a_i}{2a_r} - \frac{K}{2m^4 a_r}, \quad (32)$$

$$\beta_3 > \frac{a_r}{2a_i} - \frac{J}{2m^4 a_i}. \quad (33)$$

The normalized eigenfunction and probability density function acquire the following form:

$$\psi(x) = \sqrt{\alpha_1 \beta_1} \exp \left[\left\{ \left(\frac{1}{2} + i\beta_3 \right) a - \frac{J - iK}{2m^4} \right\} x + i\beta_3 e^{-ax} \right], \quad (34)$$

$$\psi^*(x_1, p_2) \psi(x_1, p_2) = \alpha_1 \beta_1 \exp[-2\{\alpha_1 |x_1| + \beta_1 |p_2|\}]. \quad (35)$$

5 Analysis of eigenvalues and eigenfunctions for the general case of position-dependent complex mass

To study the nature of eigenfunctions and eigenvalues admitted by the PDCM, we recall that PDCM is a linear and analytical function of x satisfying the C-R equations for the real and imaginary part of the mass defined in eq.6b. The most general case of such mass profile can be expressed in the following form:

$$m_r = cx_1 - dp_2 + e_1, \quad (36a)$$

$$m_i = dx_1 + cp_2 + e_2. \quad (36b)$$

where, c , d , e_1 and e_2 are real constants.

Substituting the value of the masses the expression for the ansatz parameters β_1 , α_1 and β_3 can be obtained. These parameters can then further be substituted in equations. 32 and 33 to derive constraints on the normalization conditions of the eigenfunction. Figure 1 shows the plot of β_3 with respect to x_1 and p_2 . The plot simply reveals the possible regions in the argand plane to achieve normalized eigenfunctions of the complex Morse potential and hence gives clues to the existence of the quantum system considered.

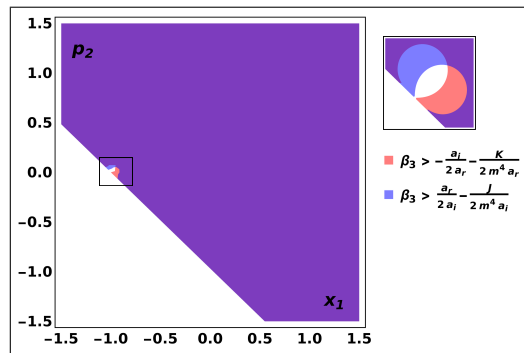


Figure 1: The Normalization condition plot for a position-dependent complex mass system. Here, the purple shade defines the intersection region of both the normalization conditions, whereas white, blue and pink shades show the region where eigenfunction can't be normalized.

On substituting the values of the real and imaginary part of the PDM defined in equations 36a and 36b into equations 25a and 25b, the real and imaginary part of the eigenvalues can be evaluated which turn out to be quite lengthy. The nature and behaviour of these eigenvalues is studied by plotting them in the Argand plane with respect to x_1 and p_2 (figures 2a and 2b).

The probability density can be evaluated from equation 35 and is plotted in figure 3a and 3b. Interestingly, the real and imaginary values of the eigenvalues of the Complex Morse potential plotted in figures 2 and 3 subscribe to the characteristics of the eigenfunction of the said potential enumerated in figure 1, where the eigenvalues are only defined in the region where the normalization conditions of the eigenfunctions are satisfied.

Figures 2a and 2b illustrate the variation of the imaginary and real part of the eigenvalue in the Argand plane as a function of x_1 and p_2 . As expected, for a PDCM system, the eigenvalues vary with position. In the region where only one normalization conditions is fulfilled, highlighted in pink and blue region in figure 1, the eigenvalue plots exhibit anomalous behavior, with the ground state energy diverging to either infinitely large positive or negative values. Figures 3c and 3d display the

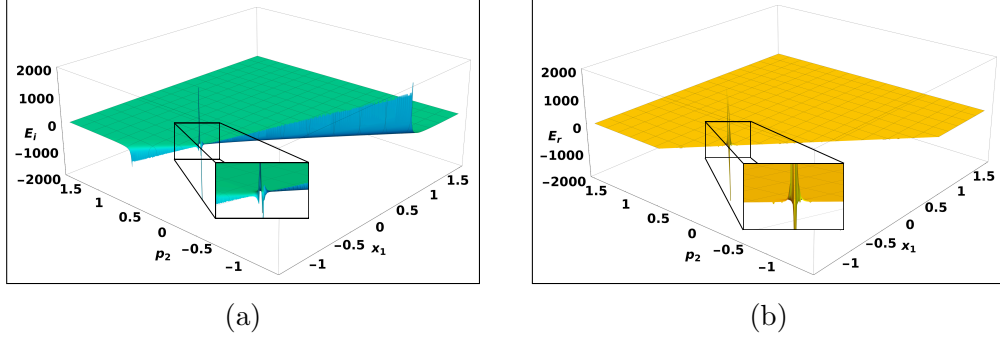


Figure 2: The eigenvalue plots of mass profile $m_r = cx_1 - dp_2 + e_1$ and $m_i = dx_1 + cp_2 + e_2$ in extended complex plane. (a) E_i Vs x_1 and p_2 plot (b) E_r Vs x_1 and p_2 .

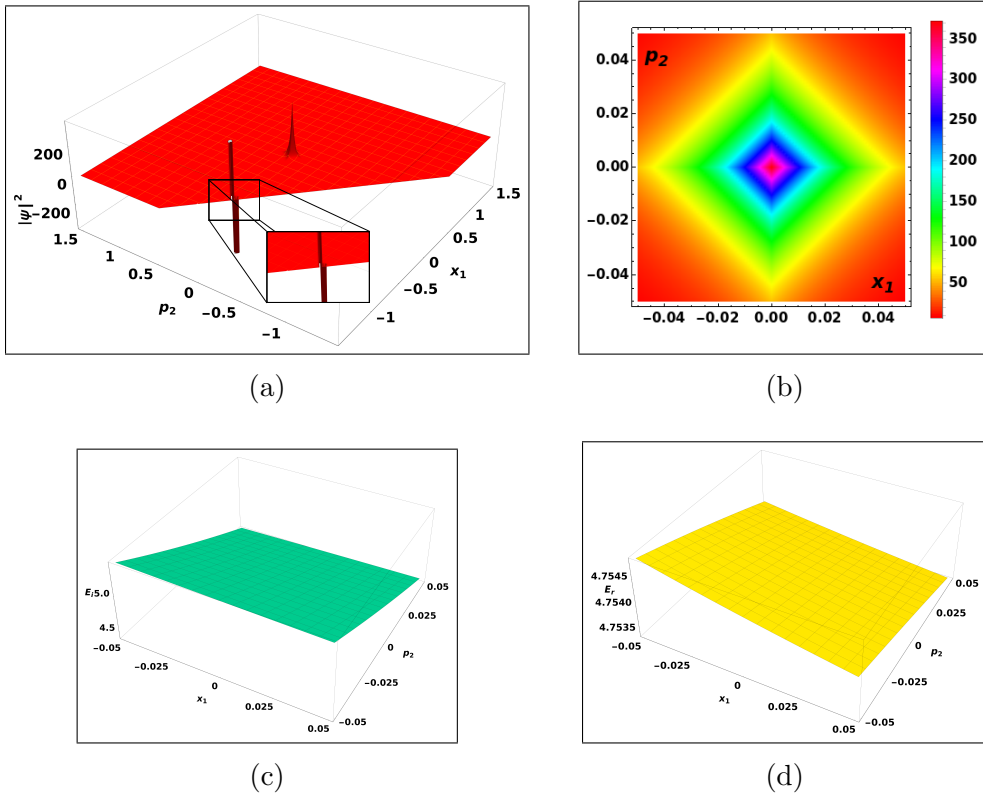


Figure 3: The general case plots for mass profile $m_r = cx_1 - dp_2 + e_1$ and $m_i = dx_1 + cp_2 + e_2$ in extended complex plane. (a) Probability density (PCD) Plot (b) Contour plot of peak in figure 3a (c) Behaviour of Imaginary part of eigenvalue at peak of PCD (d) Behaviour of real part of eigenvalue at peak of PCD.

positive ground state eigenvalue in the region corresponding to the peak observed in the probability current density plot (figure 3a). In figure 3a this region, where only a single normalization condition holds, is specifically marked, and it is noteworthy that the probability density in this area diverges to infinitely positive or negative values. The same plot also indicates the domain in which the diatomic complex system is likely to exist, as evidenced by the peak in probability current density. To further analyze this behavior, figure 3b provides a contour plot showing an increased probability of locating the particle near the origin.

5.1 Special Cases of Mass Profile

To achieve a better insight into the behaviour of the complex Morse potential with PDCM, let us analyze the special cases where masses are constant along the real or imaginary axis.

5.1.1 Case I(a), when $\frac{dm_r}{dx_1} = 0$

For the case where the real part of the PDCM does not vary along the real axis, the value of α_1 , β_1 and the general expression of real and imaginary eigenvalues are obtained as,

$$\alpha_1 = a_i\beta_3 - \frac{a_r}{2} - \frac{m_i m'_i}{2m^2}, \quad (37)$$

$$\beta_1 = a_r\beta_3 + \frac{a_i}{2} + \frac{m_r m'_i}{2m^2}, \quad (38)$$

$$E_i = \frac{1}{8m^6} \left[m^4 \left\{ (a_r^2 - a_i^2) \left((1 - 4\beta_3^2)m_i - 4\beta_3 m_r \right) - 2a_i a_r \left((1 - 4\beta_3^2)m_r + 4\beta_3 m_i \right) \right\} + (3m_r^2 m_i - m_i^3) m_i'^2 \right], \quad (39)$$

$$E_r = \frac{1}{8m^6} \left[m^4 \left\{ (a_r^2 - a_i^2) \left((4\beta_3^2 - 1)m_r - 4\beta_3 m_i \right) + 2a_i a_r \left((4\beta_3^2 - 1)m_i + 4\beta_3 m_r \right) \right\} + (3m_r m_i^2 - m_r^3) m_i'^2 \right]. \quad (40)$$

Substituting the values of α_1 and β_1 from equations 37 and 38 in equations 32, 33 and 35, the condition of normalization and probability density can be obtained. The mass function defined in equation 36a and 36b for this case is expressed in the form,

$$m_r = -dp_2 + e_1, \quad (41a)$$

$$m_i = dx_1 + e_2. \quad (41b)$$

5.1.2 Case II(a), when $\frac{dm_i}{dx_1} = 0$

Let us consider the case when the imaginary part of the mass is independent of x_1 . The values of the parameters α_1 and β_1 along with the real and imaginary parts of the eigenvalues are obtained in the following form:

$$\alpha_1 = a_i\beta_3 - \frac{a_r}{2} - \frac{m_r m'_r}{2m^2}, \quad (42)$$

$$\beta_1 = a_r\beta_3 + \frac{a_i}{2} - \frac{m_i m'_r}{2m^2}, \quad (43)$$

$$E_i = \frac{1}{8m^6} \left[m^4 \left\{ (a_r^2 - a_i^2) \left((1 - 4\beta_3^2)m_i - 4\beta_3 m_r \right) - 2a_i a_r \left((1 - 4\beta_3^2)m_r + 4\beta_3 m_i \right) \right\} - (3m_r^2 m_i - m_i^3) m_r'^2 \right], \quad (44)$$

$$E_r = \frac{1}{8m^6} \left[m^4 \left\{ (a_r^2 - a_i^2) \left((4\beta_3^2 - 1)m_r - 4\beta_3 m_i \right) + 2a_i a_r \left((4\beta_3^2 - 1)m_i + 4\beta_3 m_r \right) \right\} - (3m_r m_i^2 - m_r^3) m_r'^2 \right]. \quad (45)$$

The mass function for this case is written as,

$$m_r = cx_1 + e_1, \quad (46a)$$

$$m_i = cp_2 + e_2. \quad (46b)$$

5.1.3 Comparisons of Cases I(a) and II(a)

(i) Normalization condition

Let us compare the behaviour of particles with PDCM under the action of complex Morse potential. The expressions for the normalization condition of the eigenfunction admitted in the above mentioned special cases defined in 5.1.1 and 5.1.2 are derived and plotted in figures 4a and 4b.

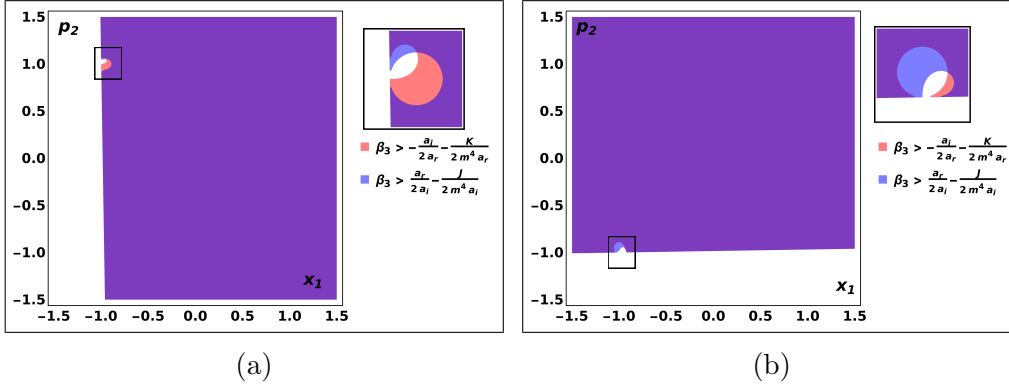


Figure 4: Normalization condition plot for (a) Case I(a) (b) Case II(a)

The comparison of the general case enumerated in figure 1 with the special cases plotted in figure 4 highlights the different regions of the Argand plane where the eigenfunction is normalized.

(ii) Behaviour of Eigenvalues

The blue and pink regions highlighted in figures 4a and 4b, which satisfy only one of the two required conditions for the existence of normalized eigenfunctions, display divergent behavior in the real and imaginary parts of the eigenvalues. This is evident from the zoomed-in views in figures 5a-5d. Therefore, the system's behavior in these regions aligns with the general case of position-dependent complex mass described by Equations 36a and 36b.

(iii) Probability density plots

The probability density plot shown in figures 7a and 7b indicates the formation of finite peaks with similar nature as in the general case. The contour plots of the region at the vicinity of the peak are demonstrated in figures 7c and 7d. The red region in the said contour plot signifies the region where the probability density is maximum and the same value decreases as one moves away from the origin. Both cases show a distinct resemblance with that of the general case (figure 3b).

(iv) Behaviour of eigenvalues at peak of probability density

Figure 6 illustrates the behavior of both the real and imaginary components of the eigenvalues in the region corresponding to the peak of the probability density function for the complex diatomic molecular system, as shown in figures 7a and 7b. It is observed that the eigenvalues are confined to a limited range of positive values.

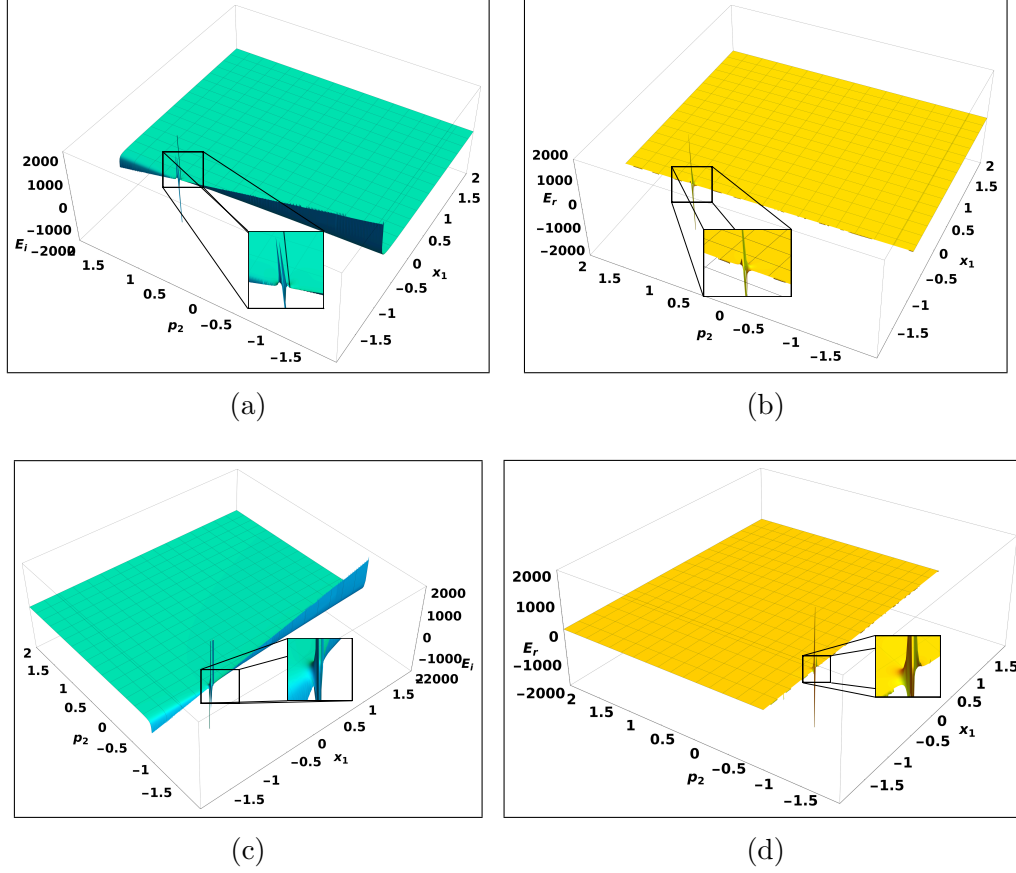


Figure 5: The eigenvalue plot for Case I(a), (a) E_i Vs x_1 and p_2 (b) E_r Vs x_1 and p_2 and Case II(a), (c) E_i Vs x_1 and p_2 (d) E_r Vs x_1 and p_2 .

6 Reality of eigenspectrum

The reality of the eigenvalue spectrum admitted by the Complex potentials has been a subject of research for the past several decades in the context of extending quantum theory beyond Hermitian operators while keeping physical observables real. The main advantage of solving the Schrödinger equation using the method described in the present study lies in the fact that the imaginary part of all physical quantities including the eigenvalues and the eigenfunction can be deduced explicitly. Equation 12a mandates that the energy eigenvalue admitted by the complex Morse potential is real for the ground state when

$$E_i(x_1, p_2) = 0. \quad (47)$$

Defining μ as $\mu = \frac{m_r}{m_i}$ and writing its first-order differential with respect to x_1 ,

$$\mu' = \frac{1}{m_i}(m_r' - \mu m_i').$$

The condition for the reality of the spectrum can be expressed as

$$\frac{(1 + \mu)m_i'}{m_i} [(\alpha_1^2 - \beta_1^2) + 2\mu\alpha_1\beta_1] \left[\frac{\mu' m_i}{m_i'} + \mu \right] [(\mu^2 - 1)\beta_1 + 2\mu\alpha_1] (\mu^2 - 1)\alpha_1 + 2\mu\beta_1 = 0. \quad (48)$$

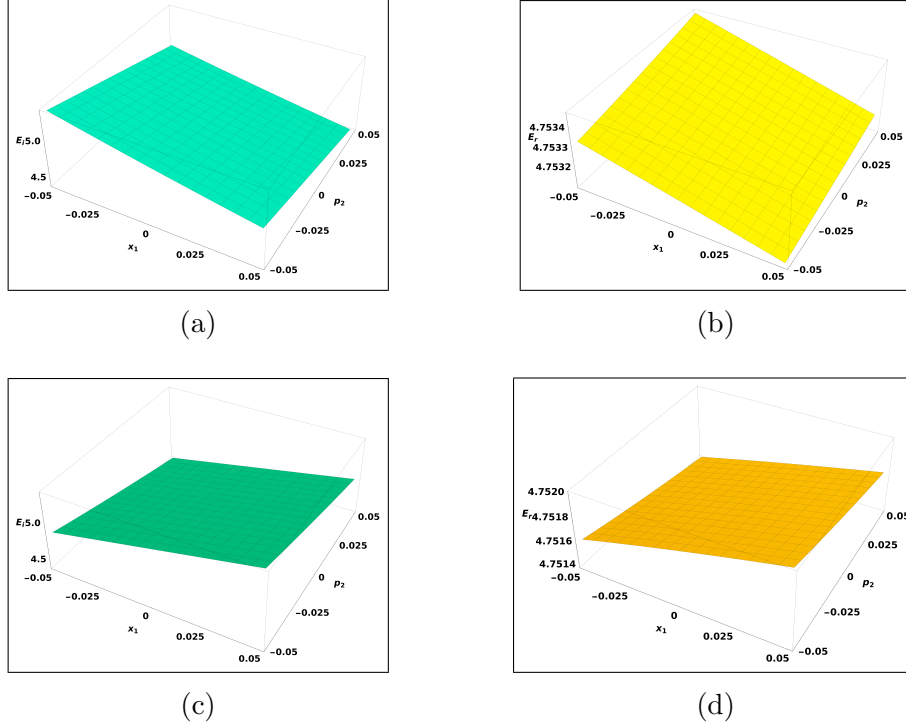


Figure 6: The eigenvalue plot of the peak for Case I(a), (a) E_i Vs x_1 and p_2 (b) E_r Vs x_1 and p_2 and Case II(a), (c) E_i Vs x_1 and p_2 (d) E_r Vs x_1 and p_2 .

By solving the constraint equation 48 using Equations 24a and 24b, the values of α_1 and β_1 are determined, which subsequently yield two distinct roots of β_3 , referred to hereafter as the first and second roots of β_3 . These roots are essential for ensuring the reality of the eigenvalue spectrum associated with the complex Morse potential. Additionally, the normalization conditions given in Equation 32 and 33 imposes further restrictions on the admissible values of β_3 , ensuring that the resulting eigenvalues are real and that the corresponding probability densities are both finite and positive. Due to their complexity, the explicit forms of these roots are too cumbersome to include in the text. Figure 8a and 8b illustrate the normalization condition plots corresponding to the two distinct roots of β_3 in the position-dependent complex mass (PDCM) system.

While real eigenvalues and probability density functions can be evaluated for both roots within the region representing the existence of a diatomic molecule, it is important to highlight that the normalization conditions given by Equations 32 and 33 are satisfied only in the purple-shaded regions of the plots, and not in the pink regions. Notably, the origin in figure 8b lies within the purple region, whereas in figure 8a, it is located in the pink region. This clearly indicates that only the second root of β_3 yields a properly normalized eigenfunction. The behavior of the corresponding real eigenvalue and probability current density for this valid root is depicted in figures 9 and 10.

To analyze the behaviour of Complex Morse potential admitting real eigenvalues, we insert the conditions imposed on the mass profiles in Cases I(a) and II(a) from the previous section.

6.1 Case I(b), $\frac{dm_r}{dx_1} = 0$

The general expression of roots of β_3 is written in the form

$$\beta_3 = \frac{m^2 \lambda_1 \mp \gamma_1}{2m^2 \lambda_2}, \quad (49)$$

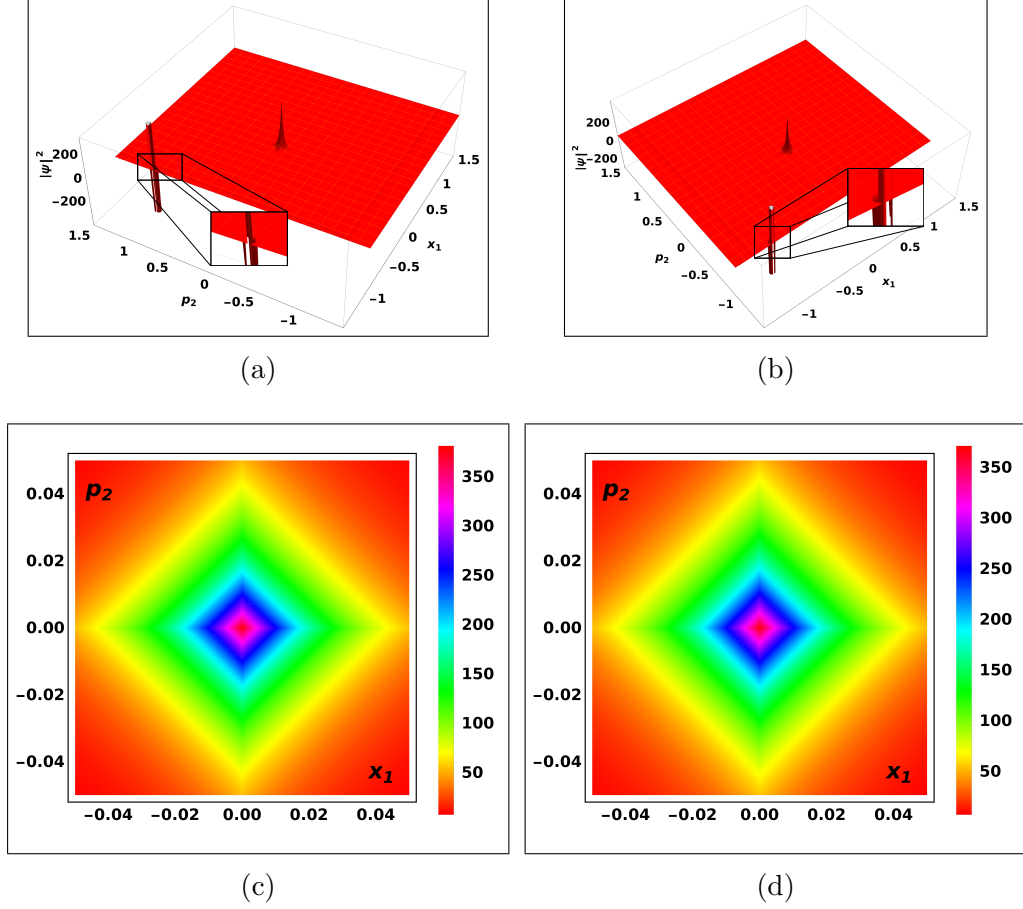


Figure 7: The probability density plots for, (a) Case I(a) (b) Case II(a) and contour plots of probability density of the peak for (c) Case I(a) (d) Case II(a)

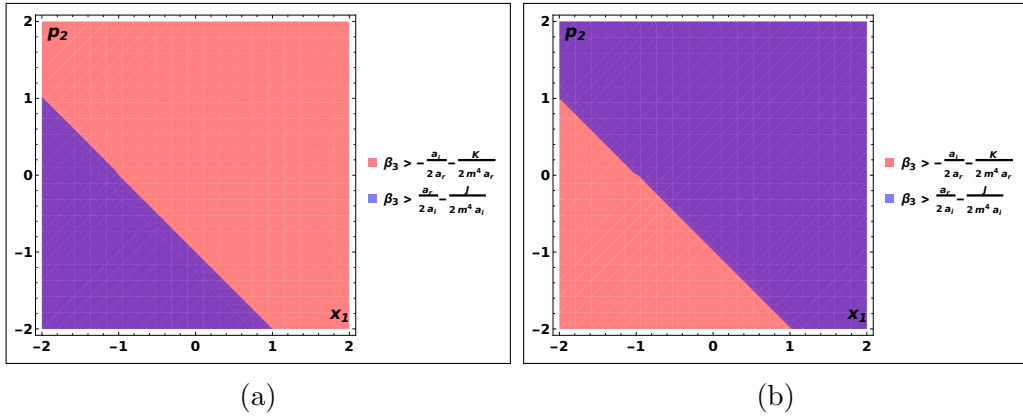


Figure 8: Normalization condition plot of reality of spectrum for mass profile $m_r = cx_1 - dp_2 + e_1$ and $m_i = dx_1 + cp_2 + e_2$ in extended complex plane associated with (a) first root of β_3 (b) second root of β_3 .

whereas, the value of α_1 and β_1 parameters take the value,

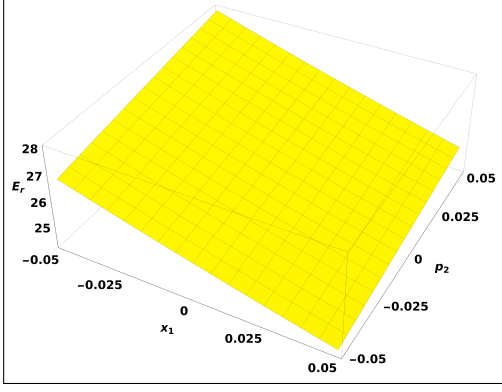


Figure 9: Real eigenvalue plot of reality of spectrum for the second root of β_3 near origin, where mass profile is $m_r = cx_1 - dp_2 + e_1$ and $m_i = dx_1 + cp_2 + e_2$ in the extended complex plane.

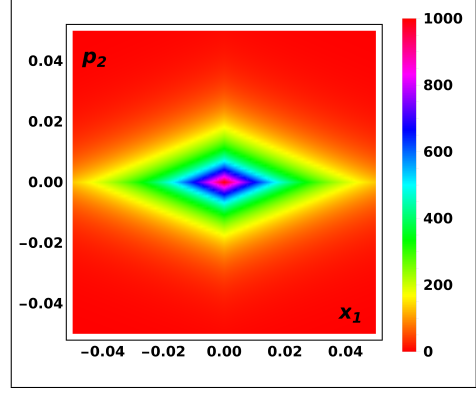


Figure 10: Probability density plot of reality of spectrum for the second root of β_3 near origin, where mass profile is $m_r = cx_1 - dp_2 + e_1$ and $m_i = dx_1 + cp_2 + e_2$ in the extended complex plane.

$$\alpha_1 = \frac{|a|^2 m^2 (m_i a_r - m_r a_i) - \lambda_2 m_i m_i' \mp a_i \gamma_1}{2m^2 \lambda_2}, \quad (50)$$

$$\beta_1 = \frac{|a|^2 m^2 (m_i a_i - m_r a_r) + \lambda_2 m_r m_i' \mp a_r \gamma_1}{2m^2 \lambda_2}. \quad (51)$$

Further, the real eigenvalue is obtained in the form,

$$E_r = \frac{(m_i^2 m_r |a|^4 + m^2 a_i a_r \lambda_3) m_i'^2 + |a|^4 m^4 \lambda_1 \mp m^2 \gamma_1}{4m^4 \lambda_2^2} \quad (52)$$

where, the variables λ_1 , λ_2 , λ_3 and γ_1 are functions of masses and dissociation parameters a defined as,

$$\lambda_1 = m_r (a_r^2 - a_i^2) + m_i (2a_i a_r), \quad (53a)$$

$$\lambda_2 = m_i (a_i^2 - a_r^2) + m_r (2a_i a_r), \quad (53b)$$

$$\lambda_3 = m_i (a_i^2 - a_r^2) - m_r (2a_i a_r). \quad (53c)$$

$$\gamma_1 = \sqrt{|a|^4 m^6 + \lambda_2 (m_i^2 - 3m_r^2) m_i m_i'}. \quad (54)$$

Figures 11a and 11b present the plots of the normalization conditions to identify the permissible values of β_3 for this scenario. It is clearly observed that the first root of β_3 corresponds to a region near the origin where the eigenfunction is properly normalized. Additionally, the behavior of the real eigenvalue and the associated probability density is illustrated in figures 12 and 13, providing further insight into the physical characteristics of the system.

6.2 Case II(b), $\frac{dm_i}{dx_1} = 0$

Similar to above case, the value of parameters and eigenvalue is deduced as,

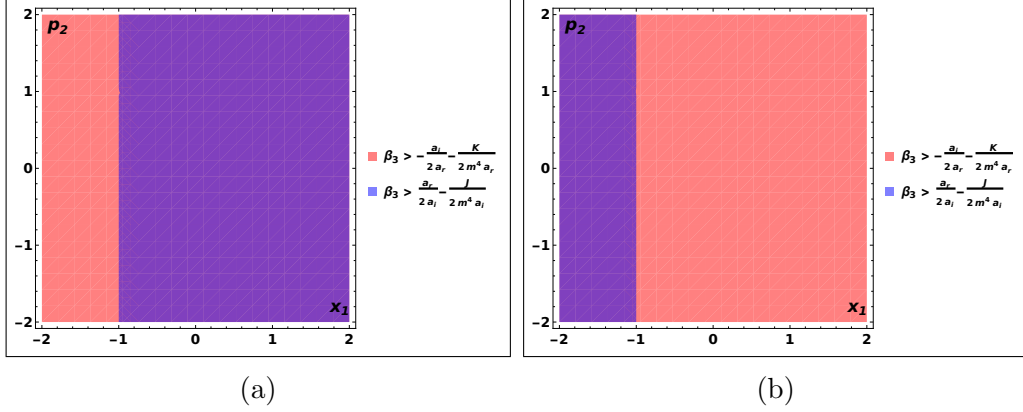


Figure 11: Normalization condition plot of reality of spectrum for Case I(b) in extended complex plane associated with (a) first root of β_3 (b) second root of β_3 .

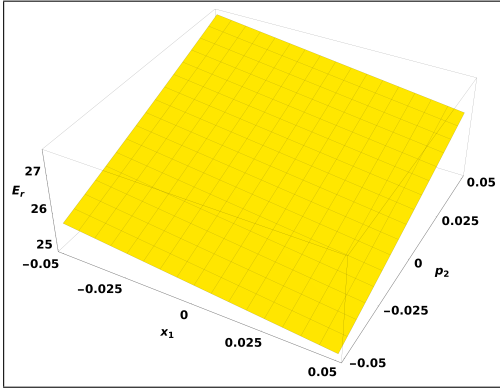


Figure 12: Real eigenvalue plot of Case I(b) for the first root of β_3 near origin in the extended complex plane.

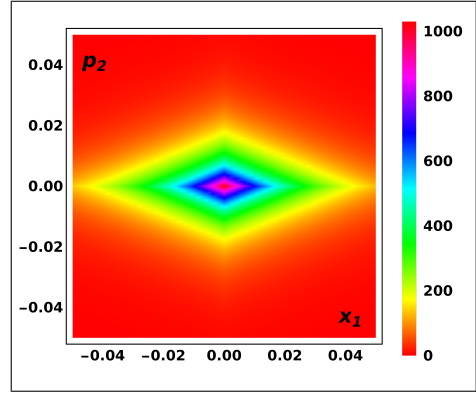


Figure 13: Probability density plot of Case I(b) for the first root of β_3 near origin in the extended complex plane.

$$\beta_3 = \frac{m^2 \lambda_1 \mp \gamma_2}{2m^2 \lambda_2}, \quad (55)$$

$$\alpha_1 = \frac{|a|^2 m^2 (m_i a_r - m_r a_i) - \lambda_2 m_r m_r' \mp a_i \gamma_2}{2m^2 \lambda_2}, \quad (56)$$

$$\beta_1 = \frac{|a|^2 m^2 (m_i a_i + m_r a_r) - \lambda_2 m_i m_r' \mp a_r \gamma_2}{2m^2 \lambda_2}, \quad (57)$$

$$E_r = \frac{-(m_i^2 m_r |a|^4 + m^2 a_i a_r \lambda_3) m_r'^2 + |a|^4 m^4 \lambda_1 \mp m^2 \gamma_2}{4m^4 \lambda_2^2}. \quad (58)$$

Where all the λ parameters are the same as enumerated in equations 53a-53b while γ_2 will be written as

$$\gamma_2 = \sqrt{|a|^4 m^6 - \lambda_2 (m_i^2 - 3m_r^2) m_i m_r'}. \quad (59)$$

The normalization condition plots shown in figures 14a and 14b clearly indicate that the second root of β_3 satisfies the normalization criteria in the region near the origin. Correspondingly, figures 15 and 16 depict the eigenvalue and probability density within this region, illustrating the behavior of the system for this case where the energy spectrum remains real.

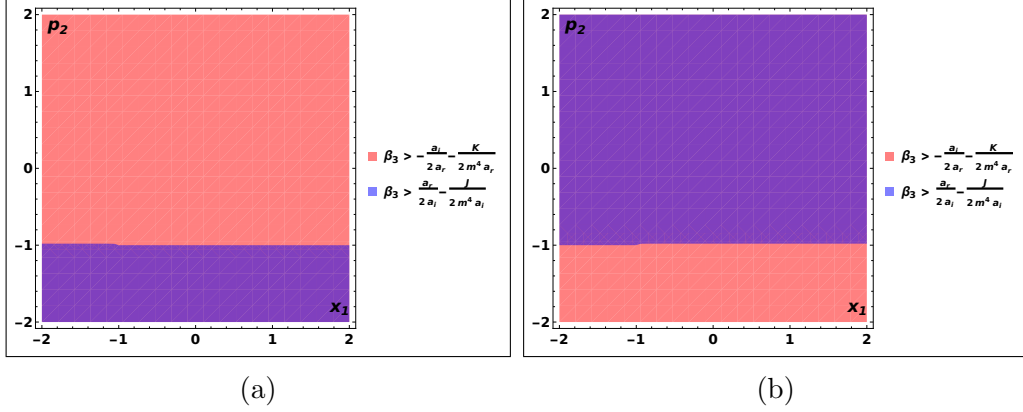


Figure 14: Normalization condition plot of reality of spectrum for Case II(b) in extended complex plane associated with (a) first root of β_3 (b) second root of β_3 .

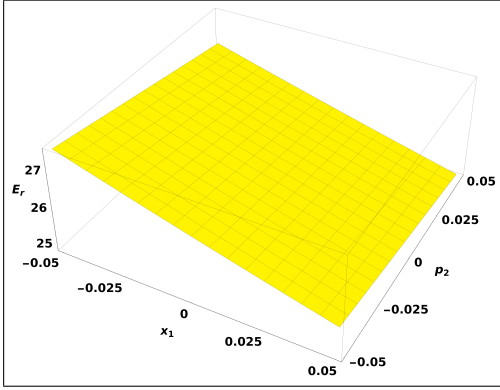


Figure 15: Real eigenvalue plot of Case II(b) for the second root of β_3 near origin in the extended complex plane.

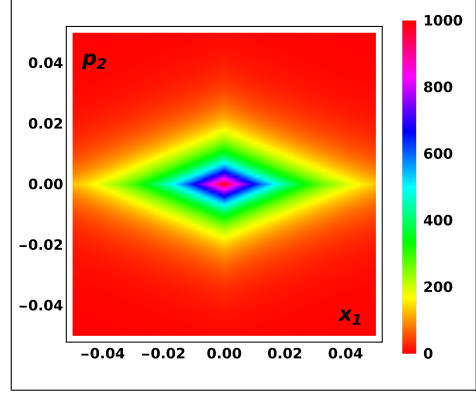


Figure 16: Probability density plot of Case II(b) for the second root of β_3 near origin in the extended complex plane.

7 Conclusion

In this study, we have analyzed the complex Morse potential with position-dependent mass (PDM) by solving the corresponding position-dependent mass Schrödinger equation (PDMSE). We derived the eigenvalues and eigenfunctions and addressed the critical aspect of normalization. Due to the non-Hermitian nature of complex potentials and the variable mass distribution, the eigenfunctions are generally not square-integrable in the traditional sense. Therefore, we adopted a modified normalization condition defined as a two-dimensional integral over the phase space:

$$\int_{-\infty}^{\infty} \int_{-\infty}^{\infty} \psi^*(x_1, p_2) \psi(x_1, p_2) dx_1 dp_2 = \text{constant}.$$

The convergence of this integral is essential for maintaining the probabilistic interpretation of quantum mechanics. A key achievement of the present study was the formulation of an appropriate normalization condition suited to complex systems with PDM. Using this criterion, the normalized eigenfunction was obtained (as shown in Equation 34), with the normalization constant evaluated in Equation 31 under the constraints specified in Equations 32 and 33. This ensures the physical validity of the wavefunctions, enabling stable, interpretable, and physically meaningful expectation

values.

Our analysis demonstrates that, under suitable parameter constraints, the Complex Morse Potential with PDM can support real eigenvalues—an essential requirement for observable physical quantities. The probability density plots (figures 3a, 7a and 7b) exhibit finite peaks in phase space, indicating that the bound states are localized, and particles remain confined to specific regions. These results confirm that the system supports stable, localized bound states and preserves many qualitative features of the real Morse potential.

Furthermore, our findings underscore a significant point: the reality of the energy spectrum is more fundamental than the Hermiticity of the Hamiltonian. The complex Morse system with PDM can exhibit real eigenspectra due to underlying symmetries or parameter conditions, even when the Hamiltonian itself is non-Hermitian. Complex potentials with PDM are analogous to refractive index profiles in PT-symmetric optical systems. Our findings could inform the design of optical lattices or waveguides. Since many open systems are inherently non-Hermitian, the framework developed here can model gain-loss systems, decoherence, or energy dissipation [73–77]. Finally, we speculate that such systems may have deeper implications in high-energy or cosmological contexts [64, 66]. The complex Morse potential with position-dependent mass may provide a theoretical framework for describing exotic quantum systems such as dark matter. Given that dark matter constitutes a significant portion of the Universe, our model suggests that bound states governed by complex PDM potentials could offer insight into its quantum behaviour. These findings also raise the possibility that visible matter emerged via phase transitions or symmetry breaking, leading to effective real Morse-like potentials in the post-early-Universe evolution.

The methods and insights presented here contribute meaningfully to the growing body of literature on non-Hermitian quantum mechanics and provide a viable quantum model for systems with position-dependent complex mass, a concept that could play crucial role in both fundamental physics and applied quantum physics.

References

- [1] Kato T 2013 *Perturbation Theory for Linear Operators* vol 132 (Springer Science & Business Media)
- [2] Davies E B 2007 *Linear Operators and Their Spectra* vol 106 (Cambridge University Press)
- [3] Bender C M and Boettcher S 1998 *Physical Review Letters* **80** 5243
- [4] Mostafazadeh A 2002 *Journal of Mathematical Physics* **43** 205–214
- [5] Gelfand I M and Vilenkin N Y 1964 *Generalized Functions, vol. 4: Applications of Harmonic Analysis* (Academic Press)
- [6] Reed M and Simon B 1978 *IV: Analysis of Operators* vol 4 (Elsevier)
- [7] Strauss W A 2007 *Partial Differential Equations: An Introduction* (John Wiley & Sons)
- [8] Dekar L, Chetouani L and Hammann T F 1998 *Journal of Mathematical Physics* **39** 2551–2563
- [9] Yu J and Dong S H 2004 *Physics Letters A* **325** 194–198
- [10] Alhaidari A 2002 *Physical Review A* **66** 042116
- [11] Mirabotalebi S and Salehi H 2006 *General Relativity and Gravitation* **38** 269–277

- [12] von Roos O 1983 *Physical Review B* **27** 7547
- [13] von Roos O and Mavromatis H 1985 *Physical Review B* **31** 2294
- [14] Zhu Q G and Kroemer H 1983 *Physical Review B* **27** 3519
- [15] Weishbuch C and Vinter B 1993 Quantum semiconductor heterostructure
- [16] El-Nabulsi R A 2020 *Physica E: Low-dimensional Systems and Nanostructures* **124** 114295
- [17] El-Nabulsi R A 2020 *Journal of Physics and Chemistry of Solids* **140** 109384
- [18] Bastard G 1988 *Wave Mechanics Applied to Semiconductor Heterostructures* Monographies de physique (Les Editions de Physique) ISBN 9782868830920 URL <https://books.google.co.in/books?id=-jQbAQAIAAJ>
- [19] Harrison P and Valavanis A 2016 *Quantum wells, wires and dots: theoretical and computational physics of semiconductor nanostructures* (John Wiley & Sons)
- [20] Wibawa B S H, Suparmi A, Cari C, Harjana H, Sulaksono A and Permatihati L K 2024 *The European Physical Journal Plus* **139** 503
- [21] Li T L and Kuhn K J 1993 *Physical Review B* **47** 12760
- [22] Rajashabala S and Navaneethakrishnan K 2006 *Modern Physics Letters B* **20** 1529–1541
- [23] Peter A J 2009 *International Journal of Modern Physics B* **23** 5109–5118
- [24] Khordad R 2011 *Physica B: Condensed Matter* **406** 3911–3916
- [25] Kasapoglu E, Yücel M B and Duque C A 2023 *Condensed Matter* **8** ISSN 2410-3896 URL <https://www.mdpi.com/2410-3896/8/4/86>
- [26] De Saavedra F A, Boronat J, Polls A and Fabrocini A 1994 *Physical Review B* **50** 4248
- [27] Geller M R and Kohn W 1993 *Physical review letters* **70** 3103
- [28] Gora T and Williams F 1969 *Physical Review* **177** 1179
- [29] Einevoll G and Hemmer P 1988 *Journal of Physics C: Solid State Physics* **21** L1193
- [30] Morrow R A and Brownstein K R 1984 *Physical Review B* **30** 678
- [31] Bastard G 1981 *Physical Review B* **24** 5693
- [32] El-Nabulsi R A 2021 *Physica E: Low-dimensional Systems and Nanostructures* **127** 114525
- [33] Aquino N, Campoy G and Yee-Madeira H 1998 *Chemical physics letters* **296** 111–116
- [34] Bencheikh K, Berkane K and Bouizane S 2004 *Journal of Physics A: mathematical and general* **37** 10719
- [35] Alimohammadi M, Hassanabadi H and Zare S 2017 *Nuclear Physics A* **960** 78–89
- [36] de Jesus A L and Schmidt A G 2019 *Journal of Mathematical Physics* **60**
- [37] Mathews P and Lakshmanan M 1974 *Quarterly of Applied Mathematics* **32** 215–218

- [38] Carinena J, Perelomov A, Ranada M and Santander M 2008 *Journal of Physics A: Mathematical and Theoretical* **41** 085301
- [39] Ballesteros Á, Enciso A, Herranz F J, Ragnisco O and Riglioni D 2011 *International Journal of Theoretical Physics* **50** 2268–2277
- [40] Mustafa O 2021 *The European Physical Journal Plus* **136** 1–17
- [41] Quesne C and Tkachuk V 2004 *Journal of Physics A: Mathematical and General* **37** 4267
- [42] Christiansen H and Lima R 2023 *Physica Scripta* **99** 015915
- [43] Quesne C 2023 *Physica Scripta* **98** 125264
- [44] Eyube E, Notani P, Wadata U, Najoji S, Bitrus B, Yabwa D and Tanko P 2023 *Physica Scripta* **98** 095019
- [45] Bagchi B and Ghosh R 2023 *Journal of Physics: Conference Series* **2448** 012001 URL <https://dx.doi.org/10.1088/1742-6596/2448/1/012001>
- [46] Morse P M 1929 *Physical review* **34** 57
- [47] Chen G and Chen Z d 2004 *Physics Letters A* **331** 312–315
- [48] Plastino A R, Rigo A, Casas M, Garcias F and Plastino A 1999 *Physical Review A* **60** 4318
- [49] Bagchi B, Gorain P and Quesne C 2006 *Modern Physics Letters A* **21** 2703–2708
- [50] Rajbongshi H and Singh N 2015 *Theoretical and Mathematical Physics* **183** 715–729
- [51] Ikhdair S M 2012 *Molecular Physics* **110** 1415–1428
- [52] Arda A and Sever R 2011 *Communications in Theoretical Physics* **56** 51
- [53] Ovando G, Morales J and López-Bonilla J 2013 *Journal of molecular modeling* **19** 2007–2014
- [54] Moya-Cessa H M, Soto-Eguibar F and Christodoulides D N 2014 *Journal of Mathematical Physics* **55** 082103
- [55] Ganguly A, Kuru Ş, Negro J and Nieto L 2006 *Physics Letters A* **360** 228–233
- [56] Dhahbi A *et al.* 2019 *Journal of Applied Mathematics and Physics* **7** 1013
- [57] Ikot A, Okon I, Okorie U, Omugbe E, Abdel-Aty A H, Obagboye L, Ahmadov A, Okpara N, Duque C, Abdullah H Y *et al.* 2024 *Zeitschrift für angewandte Mathematik und Physik* **75** 18
- [58] Kaushal R *et al.* 2002 *Journal of physics A: Mathematical and General* **35** 8743
- [59] Kaushal R *et al.* 2003 *Physica Scripta* **68** 115
- [60] Parashar D, Kaushal R *et al.* 2004 *Journal of Physics A: Mathematical and General* **37** 781
- [61] Chand F, Singh R M, Kumar N and Mishra S 2007 *Journal of Physics A: Mathematical and Theoretical* **40** 10171
- [62] Singh R M, Chand F and Mishra S 2009 *Pramana* **72** 647–654

- [63] Singh R M, Bhardwaj S and Mishra S 2013 *Computers & Mathematics with Applications* **66** 537–541
- [64] Sarathi P and Pathak N K 2021 *Journal of Physics Communications* **5** 065006
- [65] Yeşiltaş Ö and Kouachi I I 2023 *Physica Scripta* **98** 075219
- [66] Borzou A 2021 *Journal of Cosmology and Astroparticle Physics* **2021** 023
- [67] Jamieson D and Loverde M 2020 *Physical Review D* **102** 123546
- [68] Perelstein M and Shakya B 2011 *Physical Review D—Particles, Fields, Gravitation, and Cosmology* **83** 123508
- [69] Jamieson D and Loverde M 2021 *Phys. Rev. D* **103**(10) 103522 URL <https://link.aps.org/doi/10.1103/PhysRevD.103.103522>
- [70] Brax P, van de Bruck C and Trojanowski S 2022 *Phys. Rev. D* **105**(10) 103015 URL <https://link.aps.org/doi/10.1103/PhysRevD.105.103015>
- [71] Tomilchik L M and Kudryashov V V 2005 Conformally flat metric, position-dependent mass and cold dark matter (*Preprint gr-qc/0507090*) URL <https://arxiv.org/abs/gr-qc/0507090>
- [72] Xavier Jr A L and de Aguiar M A 1996 *Annals of Physics* **252** 458–478 ISSN 0003-4916 URL <https://www.sciencedirect.com/science/article/pii/S0003491696901414>
- [73] Rüter C E, Makris K G, El-Ganainy R, Christodoulides D N, Segev M and Kip D 2010 *Nature physics* **6** 192–195
- [74] Musslimani Z H, Makris K G, El-Ganainy R and Christodoulides D N 2008 *Physical Review Letters* **100** 030402
- [75] Dey S, Raj A and Goyal S 2019 *Physics Letters A* **383** 125931
- [76] El-Ganainy R, Makris K G, Khajavikhan M, Musslimani Z H, Rotter S and Christodoulides D N 2018 *Nature Physics* **14** 11–19
- [77] Peng Q, Jiao B, Yu H, Sun L, Zhang H, Li J and Luo L 2025 *Physical Review Research* **7** 023045